SCIENTIA PLENA
www.scientiaplena.org.br
VOL. 22, NUM. 09 2026
doi: 10.14808/sci.plena.2026.094601

Nova pentadienona *O*-glicosilada como candidata antitumoral: avaliação da citotoxicidade, indução de apoptose e estudos de modelagem teórica

New *O*-glycosylated pentadienone as an antitumor candidate: cytotoxicity evaluation, apoptosis induction, and theoretical modeling studies

C. P. Gonçalves[1,2]*; D. G. G. Rando[3]; R. M. Cogo[3]; M. D. Pereira[3]; G. F. de Souza[4]; K. de M. Galvão[5]; A. O. Ribeiro[2]

[1]*Departamento de Ciências Farmacêuticas/Laboratório de Insumos Naturais e Sintéticos/Grupo de Pesquisas Químico-Farmacêuticas da UNIFESP, Universidade Federal de São Paulo, 09913-030, Diadema-SP, Brasil*
[2]*Centro de Ciências Naturais e Humanas, Universidade Federal do ABC, 09210-580, Santo André-SP, Brasil*
[3]*Departamento de Biologia Química/ Laboratório de Insumos Naturais e Sintéticos/Grupo de Pesquisas Químico-Farmacêuticas da UNIFESP, Universidade Federal de São Paulo, 09913-030, Diadema-SP, Brasil*
[4]*Departamento de Ciências Biológicas, Instituto Universitario Italiano de Rosario, Corrientes 720, PB y 1er Piso Rosario S2000CTT, Santa Fe, Argentina*
[5]*Curso de Medicina do Centro Universitário das Américas – FAM, 01304-001, São Paulo-SP, Brasil*

**carolina.passarelli@unifesp.br*
(Recebido em 22 de dezembro de 2025; aceito em 21 de setembro de 2026)

O câncer de mama permanece como uma das principais causas de mortalidade entre mulheres, reforçando a necessidade do desenvolvimento de novos agentes antitumorais eficazes e seguros. A curcumina apresenta limitações farmacocinéticas que restringem sua aplicação clínica, motivando a obtenção de novos análogos estruturais. Neste estudo, avaliou-se a atividade antitumoral *in vitro* de uma nova pentadienona *O*-glicosilada (composto *9*), derivada da curcumina, frente à linhagem de adenocarcinoma mamário humano MCF-7. A citotoxicidade foi determinada pelo ensaio do MTT, enquanto os mecanismos celulares associados foram investigados por análise do ciclo celular, potencial de membrana mitocondrial (ΔΨm) e liberação de citocromo c por citometria de fluxo. Adicionalmente, modelagem molecular, análise de potencial eletrostático e uma abordagem exploratória de *target fishing* foram empregados para correlacionar propriedades estruturais e eletrônicas com a atividade biológica observada. O composto *9* apresentou atividade citotóxica moderada contra células MCF-7 (CI_{50} = 14,94 µM). Valores de CI_{50} relatados para a curcumina em células MCF-7 variam de acordo com as condições experimentais e são apresentados aqui para fins de contextualização. A redução do ΔΨm e o aumento da liberação de citocromo c foram compatíveis com participação da via mitocondrial da apoptose. Em FN-1, o composto apresentou CI_{50} = 6,05 µM e índice de seletividade de 0,40, evidenciando baixa seletividade tumoral. O *target fishing* sugeriu possíveis associações com alvos envolvidos em migração celular e angiogênese, como o eixo CXCL12. Em conjunto, o composto *9* constitui um protótipo molecular citotóxico que requer otimização estrutural para melhorar a seletividade tumoral.
Palavras-chave: pentadienona, câncer de mama, apoptose mitocondrial.

Breast cancer remains one of the leading causes of cancer-related mortality among women, highlighting the need for new antitumor agents with improved efficacy and safety profiles. Curcumin exhibits pharmacokinetic limitations that hinder its clinical application, motivating the development of new structural analogues. In this study, the *in vitro* antitumor activity of a new *O*-glycosylated pentadienone (compound *9*), derived from curcumin, was evaluated against the human breast adenocarcinoma cell line MCF-7. Cytotoxicity was assessed using the MTT assay, while the associated cellular mechanisms were investigated through cell cycle analysis, mitochondrial membrane potential (ΔΨm) disruption, and cytochrome c release by flow cytometry. In parallel, theoretical molecular modeling, electrostatic potential analysis, and an exploratory target fishing approach were employed to correlate structural and electronic features with the observed biological effects. Compound *9* exhibited moderate cytotoxic activity against MCF-7 cells (IC_{50} = 14.94 µM). Reported IC_{50} values for curcumin in MCF-7 cells vary according to experimental conditions and are presented here for contextual purposes. ΔΨm reduction and increased cytochrome c release were consistent with mitochondrial apoptotic pathway involvement. In FN-1 fibroblasts, compound 9 showed IC_{50} = 6.05 µM and a selectivity index of 0.40, indicating low tumor selectivity. Target fishing analysis suggested potential associations with targets involved in cell migration and angiogenesis, such as the CXCL12 axis. Overall, compound *9* represents a cytotoxic molecular prototype requiring structural optimization to improve tumor selectivity.
Keywords: pentadienone, breast cancer, mitochondrial apoptosis.

1. INTRODUCTION

Breast cancer remains one of the leading oncological challenges worldwide, accounting for a high mortality rate among women in several regions. Despite the wide range of available treatments, including chemotherapy, hormone therapy, and immunotherapy, many patients continue to experience therapeutic resistance, systemic side effects, and recurrence, particularly in the more aggressive forms of the disease [1]. The urgent demand for more selective antitumoral agents, with innovative mechanisms of action and lower toxicity toward normal cells, has driven the search for new bioactive compounds of both natural and synthetic origin [2].

Curcumin, a polyphenol found in the rhizomes of *Curcuma longa*, has been extensively studied for its antioxidant, anti-inflammatory, and antitumoral properties against several tumor lines. However, despite its promising therapeutic potential against various tumor cell lines, curcumin exhibits serious pharmacokinetic limitations, such as poor water solubility, rapid metabolic degradation, and limited systemic bioavailability, which compromises its clinical effectiveness. To overcome these drawbacks, several chemical strategies have been employed, including the synthesis of more stable structural analogs with enhanced capacity to interact with molecular targets involved in tumor progression [3, 4].

Among these derivatives, pentadienone-type compounds, retaining curcumin's central scaffold, have shown an increase in cytotoxic potency, particularly following structural modifications such as methoxylation, acylation, and more recently, glycosylation [5, 6]. The incorporation of carbohydrate residues into bioactive molecules is an approach aimed not only at improving pharmacokinetic properties such as solubility and bioavailability, but also at enhancing selective recognition by tumor cells, given the differential expression of lectin and glycoprotein receptors in neoplastic membranes [7].

Compound *9* (1*E*,4*E*)-1-(4-((3*R*,4*S*,5*R*)-3,4,5-tris(benzyloxy)-tetrahydro-6-methyl-2*H*-pyran-2-yloxy)-3-methoxyphenyl)-5-(4-((3*S*,4*R*,5*S*)-3,4,5-tris(benzyloxy)-tetrahydro-6-methyl-2H-pyran-2-yloxy)-3-methoxyphenyl)penta-1,4-dien-3-one, the focus of the present study, is an *O*-glycosylated pentadienone derivative obtained through targeted structural modifications of curcumin. Compound 9 was selected for the present study to investigate the biological effects associated with the introduction of carbohydrate moieties into the curcumin-derived pentadienone scaffold. Considering that glycoconjugates exhibit affinity for lipid microdomains of cell membranes and can modulate intracellular signaling pathways associated with apoptosis, proliferation, and immune recognition, their cytotoxic activity and cellular mechanisms related to programmed cell death were investigated. The MCF-7 human breast adenocarcinoma cell line was selected as the experimental model due to its clinical relevance and its widespread use in antineoplastic compound screening assays [8].

In addition to conventional biological assays, a complementary theoretical modeling approach was employed to investigate the conformational, electronic, and electrostatic potential properties of the new molecule, enabling the establishment of correlations between its chemical structure and biological activity. The results obtained provide relevant insights into the apoptotic mechanisms triggered by compound *9*, particularly those associated with the intrinsic mitochondrial pathway. Considering the low selectivity observed for compound 9, these findings should be interpreted as an initial characterization of a molecular prototype with cytotoxic activity that requires structural optimization.

Therefore, we hypothesized that *O*-glycosylation of a curcumin-derived pentadienone scaffold could modulate cytotoxicity and mitochondrial apoptosis-related events. This study aimed to evaluate the cytotoxic profile of compound 9 in MCF-7 tumor cells and non-tumoral FN-1 fibroblasts and J774 macrophages, and to investigate cell-cycle alterations, mitochondrial membrane potential, cytochrome c release, and theoretical electronic properties of compound *9* in breast cancer MCF-7 cells.

2. MATERIAL AND METHODS

All reagents used in this study were purchased from Sigma Chemical Co. (St. Louis, MO, USA), including RPMI-1640 medium, heat-inactivated fetal bovine serum, glutamine, garamycin, propidium iodide, ribonuclease-A, and acidified isopropanol, as well as the dyes and antibodies used in flow cytometry analyses, such as Rhodamine 123 (Invitrogen), FITC-conjugated anti-cytochrome c antibody (Santa Cruz, CA, USA), PE-labeled anti-human antibody, and isotype control IgG (B.D. Biosciences). The MCF-7 cell line was used as a tumor model, alongside control cells including normal human fibroblasts (FN-1) and macrophages (J774). MCF-7 cells were obtained from the American Type Culture Collection (ATCC), whereas FN-1 fibroblasts and J774 macrophages were obtained from the Instituto Butantan (São Paulo, Brazil). Theoretical studies were conducted using Gaussian 09W and GaussView 5.0 software, with licenses obtained through FAPESP (Grant No. 2013/01875-0) and CAPES (DotLib access). Molecular file conversions were performed using the OpenBabel software. Flow cytometry analyses were carried out using FACScan and FACSCalibur instruments (Becton Dickinson, San Jose, CA, USA), with data acquisition and processing performed using CellQuest and ModFit 2.9 software.

2.1 Cytotoxicity MTT assay

The cell lines were routinely cultured in RPMI-1640 medium containing 10% inactivated fetal bovine serum (supplemented with 2.0 mM glutamine and 50 μg/mL garamycin) at 37 °C in a humidified incubator with 5% CO_2. The cells (1 × 104/well) in 96-well plates were treated with various concentrations of the different treatment groups. The cells were treated with compound *9* from 0.03 μM to 15.5 μM for 24 h, and the cell viability was assessed by the MTT assay. The cell viability was determined by MTT [3-(4,5-dimethylthiazol-2-yl)-2,5-diphenyl tetrazolium bromide] method. At the end of the treatment, MTT (0.5 mg/mL) was added to a fresh medium. After 4 h of incubation, the blue formazan crystals were dissolved with 100 μL acid-isopropanol and the absorbance was measured at 570 nm using a microplate reader. All experiments were performed in triplicate, with untreated cells serving as the control group. IC_{50} values were estimated from the concentration–response data obtained in the MTT assay.

2.2 Cell cycle analysis

MCF-7 and normal FN-1 cells were treated for 6 h with compound *9*. The control cells were treated with PBS alone. Supernatant and adherent cells were collected and washed in PBS. Cells and apoptotic bodies were harvested by centrifugation at 3000 rpm for 10 min. The cell pellet was fixed in ice-cold ethanol (70%) and maintained overnight at −20 °C. Before analysis, PBS containing 1.8 μg/mL propidium iodide and 0.1 mg/L ribonuclease-A was added to the cell pellet and incubated in the dark for 20 min at room temperature. At least 10,000 events were acquired using CellQuest software. The DNA content was measured in the FL2 channel on the Cytometer (FACSCalibur). The percentage of apoptotic cells and cells in the cell cycle phases G0/G1, S, G2/M, and sub-haploid cells was determined using the ModFit 2.9 software.

2.3 Mitochondrial membrane electric potential assessment by flow cytometry (ΔΨm)

The mitochondrial membrane potential (Δψm) was assessed in MCF-7 and normal cells FN-1 by flow cytometry using Rhodamine 123 (Invitrogen), a fluorescent lipophilic cationic dye, which preferentially enters mitochondria due to the highly negative mitochondrial membrane potential. The depolarization of ΔΨm results in the loss of Rhodamine-123 from the mitochondria and a decrease in intracellular fluorescence. The cells were collected after treatment, washed with PBS, and centrifuged at 1500 rpm at 4 °C for 5 min and incubated in PBS containing 0.5 μg/mL Rhodamine 123 for 10 min at 37 °C, in a humidified incubator with 5% CO_2. The data acquisition was performed by flow cytometry (FACSCalibur) and analyzed by Cell Quest software. The samples were analyzed for fluorescence using a FL-1H detector on a Becton Dickinson FACScan

flow cytometer. A total of 10,000 cells/sample was analyzed and the mean fluorescence intensity and percentage of cells in each population (M1 and M2) were recorded. Flow cytometry histograms were recorded, and the relative intensity of fluorescence was calculated as the mean of active mitochondria (viable cells) or inactive mitochondria (inviable cells) of the control and treated samples.

2.4 Flow cytometry expression of cytochrome c

The MCF-7 and normal FN-1 cells were exposed to compound *9* for 12 h and stained with PE-labeled anti-human antibody or isotype control IgG (B. D. Biosciences). The cells were first fixed and permeabilized with Triton X-100 0.02%, for 30 min before the addition of specific primary antibodies, then stained with FITC labeled anti-cytochrome c antibody or isotype control antibody (Santa Cruz, CA, USA). The percentages of cells expressing cytochrome c were determined using a FACScan flow cytometry system (Becton Dickinson, San Jose, CA).

2.5 Theoretical studies

The three-dimensional models designed for each compound were subjected to geometric optimization by molecular mechanics under the MM+ force field and, subsequently, the calculation of partial atomic charges using the PM3 semi-empirical methodology, both force field and charge calculation algorithm implemented in the Gaussian 09W software. The total energies of the energy-optimized conformers were calculated using the ab initio HF/6-31g* method and considering the distribution of electrostatic potential by employing the ChelpG charges calculation, also using the Gaussian 09W program. The files containing the three-dimensional information of each structure, as well as the charge information of the electrostatic potential of the ChelpG type, were the input files used on the electrostatic potential distribution calculations. Data of orbital energies, dipole moment partial charges, and atomic volume were used in the comparative analysis by which it was intended to carry out qualitative studies of chemical structure and biological activity (SAR).

2.6 Target fishing

Target fishing studies were performed on the web-based software Similarity ensemble approach (SEA) (https://sea.bkslab.org/) [9], where the SMILES for compound *9* was used as input. The analysis was performed considering two main parameters provided by the SEA algorithm: the P-value, which estimates the statistical significance of the similarity result, and the maximum Tanimoto coefficient (max-TC), which quantifies the degree of structural similarity between compound *9* and known ligands. Only targets presenting extremely low P-values ($P < 1 \times 10^{-10}$) were considered for further discussion. Targets were interpreted as putative and exploratory, aiming to generate hypotheses regarding possible biological pathways potentially affected by compound ***9***, rather than to define validated molecular targets.

2.7 Statistical analysis

The results were subjected to ANOVA, and the means were compared pairwise using the post-hoc Tukey test at a significance level of 95% ($p < 0.05$) with the GraphPad Prism 6 software. Values in the figures represent the mean of three experiments ± standard deviation.

3. RESULTS AND DISCUSSION

3.1 Cytotoxic Assay

Compound *9* demonstrated cytotoxic activity against the MCF-7 human breast adenocarcinoma cell line, with an IC_{50} of 14.94 μM. Although this potency falls within the micromolar range, literature-reported IC_{50} values for curcumin in MCF-7 cells vary according to the experimental model and exposure conditions. Hu et al. (2018) [10] reported an IC_{50} of 1.32 ± 0.06 μM after 72 h, whereas Zargan et al. (2022) [11] reported an IC_{50} of 78 μM after 24 h in a three-dimensional MCF-7 culture model. These values are presented here for contextual purposes. The IC_{50} value observed for normal human fibroblasts (FN-1) was 6.05 μM, indicating that further refinement is needed to improve tumor selectivity. Nevertheless, the cytotoxic profile of compound 9 offers a valuable starting point for optimization. The presence of a carbohydrate moiety may influence interactions with carbohydrate-binding proteins and membrane-associated recognition processes, which are known to participate in cancer-related cellular signaling [12]. These features suggest a hypothesis of potential selective uptake or binding; however, this possibility was not directly tested in the present study (Table 1).

Table 1: IC_{50} value (μM) of compound 9 against MCF-7 tumor cells and normal human fibroblasts (FN-1) after 24 h of treatment using the MTT assay. The Selectivity Index (SI) was calculated as $SI = IC_{50}(FN\text{-}1)/IC_{50}(MCF\text{-}7)$.

Compound	MCF-7 (μM)	FN-1 (μM)	SI
9	14.94	6.05	0.40

The low selectivity index (SI < 1) indicates preferential toxicity toward normal fibroblasts, suggesting that compound *9* lacks tumor selectivity at the tested concentrations. This behavior may hypothetically be related to its high lipophilicity and steric bulk associated with the benzyl-protected glycosidic moiety, which could favor nonspecific membrane interactions and passive cellular uptake; however, this hypothesis was not directly tested. These results highlight the need for further structural optimization, particularly aimed at reducing lipophilicity and improving selective recognition of tumor cells. Because the selectivity index is below 1, compound *9* was more cytotoxic to FN-1 fibroblasts than to MCF-7 cells under the tested conditions; the compound's favorable chemical features, tractable scaffold, and demonstrable cytotoxicity justify continued investigation. Further studies involving structural analogues, mechanistic evaluations (e.g., apoptosis induction, cell cycle arrest), and targeted delivery approaches may enhance its therapeutic profile and expand its applicability to breast cancer treatment. Recent studies on curcumin analogues have emphasized that structural modification of the parent scaffold can modulate anticancer activity, pharmacokinetic properties, and selectivity, supporting further optimization of curcumin-derived compounds [13, 14].

3.2 Mitochondrial membrane electric potential assessment by flow cytometry (ΔΨm)

Mitochondria are highly dynamic organelles that play a central role in the regulation of apoptotic cell death. A reduction in mitochondrial membrane potential (ΔΨm) is a well-established hallmark of the intrinsic apoptotic pathway. In this study, ΔΨm was assessed by Rhodamine 123 staining and analyzed by flow cytometry [15]. The cellular uptake of Rhodamine 123 was compared between MCF-7 breast cancer cells and normal human fibroblasts (FN-1). After 6 h of treatment with compound ***9***, MCF-7 cells exhibited a significant reduction in ΔΨm relative to untreated controls, as evidenced by decreased Rhodamine 123 fluorescence and an increased proportion of cells with inactive mitochondria (M1 population). In contrast, treatment with compound *9* did not significantly alter mitochondrial membrane potential in normal human

fibroblasts, which maintained predominantly functional mitochondria, indicating preservation of mitochondrial integrity under the experimental conditions (Figure 1).

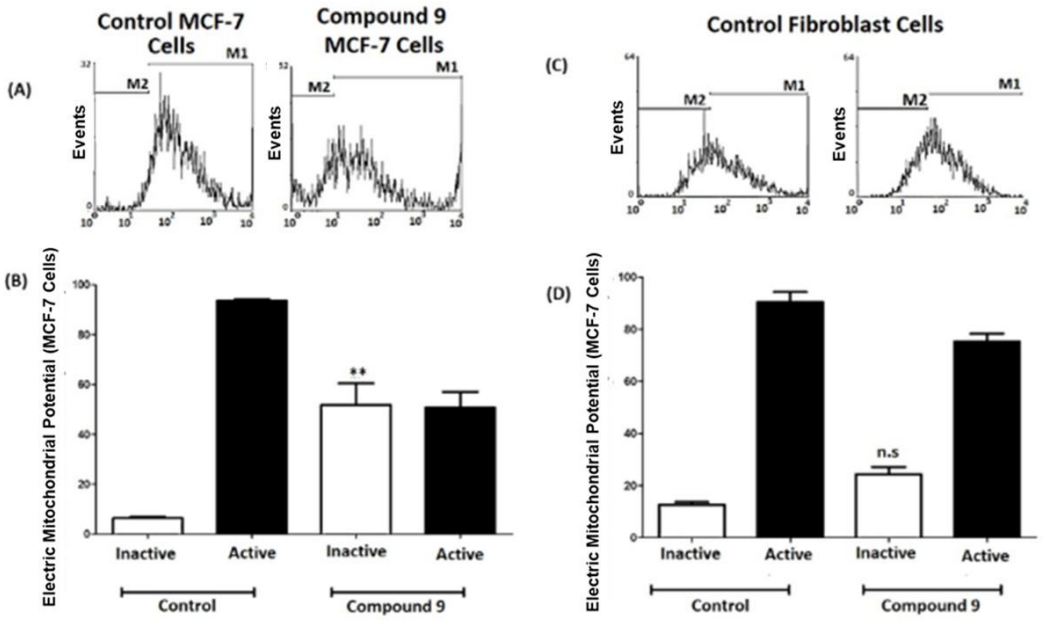


*Figure 1: Effect of compound 9 on mitochondrial membrane potential (ΔΨm) in MCF-7 cells and fibroblasts. (A) Representative histograms of control and compound 9-treated MCF-7 cells; (B) quantification of inactive and active mitochondrial potential in MCF-7 cells; (C) representative histograms of control and compound 9-treated fibroblasts; and (D) quantification of inactive and active mitochondrial potential in fibroblasts. **p < 0.01; n.s., not significant. Source: Research data.*

3.3 Flow cytometry analysis in the study of apoptosis

Cytochrome c plays an essential role in mitochondrial electron transport and intrinsic apoptosis. To further investigate mitochondrial events associated with the cellular response to compound 9, the involvement of regulatory apoptotic proteins was studied [16]. We found that cytochrome c release is significantly increased upon treatment with compound *9*, a finding compatible with involvement of the intrinsic mitochondrial apoptotic pathway, but not sufficient on its own to definitively establish apoptosis. Despite the absence of functional caspase-3 in MCF-7 cells, cytochrome c release can promote apoptosis via caspase-7 activation, as previously demonstrated in the literature. Compound *9* induces release of cytochrome c from the intermembrane mitochondrial space after 12 h of treatment, a mechanism that occurs during cell death by apoptosis by the intrinsic pathway. Treatment with compound *9* on normal human fibroblast cells did not show significant differences in the levels of cytochrome c release for cytopathic effect (Figure 2).

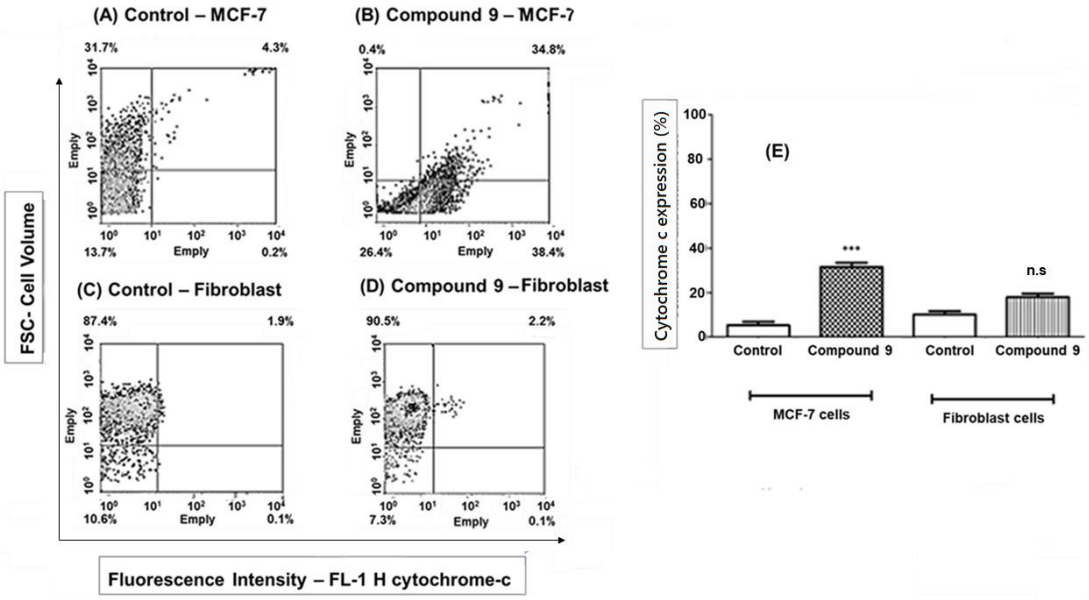


*Figure 2: Effect of compound 9 on cytochrome c expression in MCF-7 cells and fibroblasts. Representative flow cytometry plots of (A) control MCF-7 cells, (B) compound 9-treated MCF-7 cells, (C) control fibroblasts, and (D) compound 9-treated fibroblasts. (E) Quantification of cytochrome c expression in MCF-7 cells and fibroblasts. ***p < 0.001; n.s., not significant.*

3.4 Effect of the compound *9* on the cell cycle

Compound *9* was evaluated for its ability to induce changes in the cell cycle. The MCF-7 tumor and fibroblast normal cells were treated with compound *9* at a concentration of 14.94 μM and 6.05 μM, respectively, for 6 h. The exposure time was determined by considering the results of the cytotoxicity. The distribution of MCF-7 tumor cells treated with compound *9* showed significant alterations compared to the control group, including an arrest in the G2/M phase and an increase in DNA fragmented cells. G2/M arrest is consistent with DNA damage response or microtubule disturbance. Considering the planar aromatic system of compound *9*, interaction with DNA or inhibition of mitotic spindle dynamics may be involved, although further assays are required. The number of cells in the G0/G1 phase was not changed by treatment with 9, compared to the control group (51.7 ± 4.7%), presenting a percentage of 56.2 ± 8.2 by compound *9* treatment. The treatment of normal human fibroblasts with compound *9* significantly increased the proportion of cells with DNA fragmented, demonstrating cytotoxic effects without cell cycle selectivity in normal fibroblasts (Figure 3).

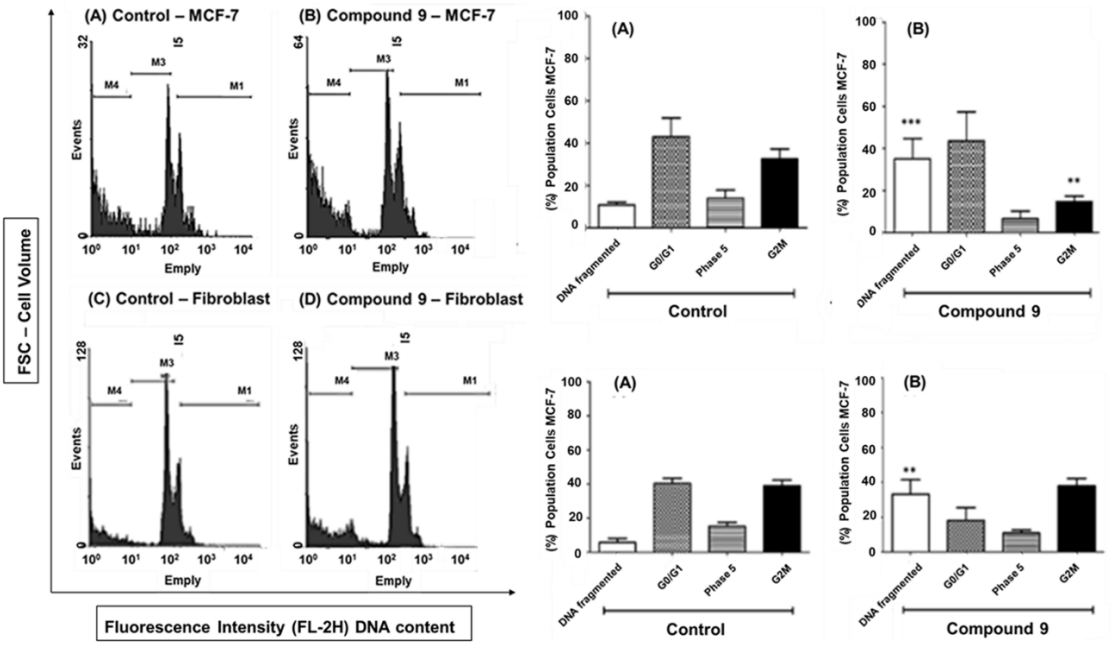


*Figure 3: Cell cycle phases histograms distribution of DNA content of MCF-7 breast cancer cells. (A and B) and FN-1 fibroblast human normal cells (C and D) following treatment with compound 9. The percentage of cells in each phase of the cell cycle (DNA fragmented (sub G1), G0/G1, S and G2/M) was quantified by flow cytometry. Bar graphs show the mean and SD of MCF-7 tumor cells (A and B) and fibroblast normal cells (C and D) treated with compound 9 and control group. All data represent the mean ± S.D. of at least three separate experiments. Significant differences from untreated controls are indicated (**p < 0.01 and ***p<0.001), obtained by the ANOVA followed by Tukey–Kramer multiple comparisons test.*

3.5 *In vitro* cytotoxicity effect in macrophages

The evaluation of compound *9* in murine macrophage (J774) cultures showed a significant increase in MTT-derived metabolic activity/viability at concentrations ranging from 15.5 to 1.93 µM. At concentrations of 0.97 µM and below, no increase in the MTT-derived signal was observed compared with untreated controls (Figure 4).

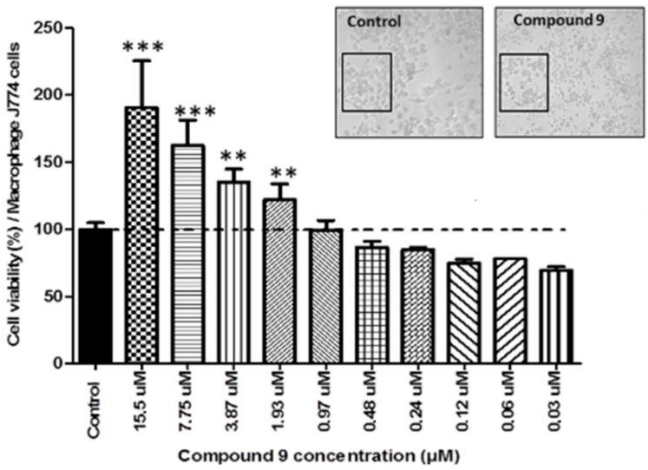


*Figure 4: Cytotoxicity assay (MTT) in macrophages of lineage J774 after 24 h treatment with compound 9. The results demonstrate that concentrations of 15.5 µM to 1.93 µM occurred a significant increase in the MTT-derived metabolic activity/viability signal. At concentrations of 0.97 µM and below, no significant increase in the MTT-derived signal was observed compared with untreated controls. **Statistical differences were determined by ANOVA followed by Tukey–Kramer multiple comparisons test (**p < 0.01; *p < 0.001).*

The increase in MTT-derived signal should be interpreted cautiously because this assay does not directly assess immune activation or proliferation. The carbohydrate moiety in compound *9* may contribute to interactions with macrophage membrane components or receptors, which may represent a hypothesis for future functional studies rather than evidence of activation or proliferation-related pathways. Given the role of macrophages in tumor surveillance and modulation of the tumor microenvironment, the observed MTT response in J774 cells should not be interpreted as a demonstrated pharmacological advantage or immunostimulatory effect. However, further studies employing specific functional and immunological markers are required to clarify the nature of the observed metabolic response.

3.6 Theoretical studies

Structurally, compound *9* is a sterically hindered molecule due to the presence of benzyl protecting groups on its glycosidic portion. Despite this, the compound tends to adopt a compact conformation. This folded geometry can be attributed to the occurrence of π-stacking interactions between the aromatic rings flanking the glycosidic region, with π–π interactions at distances consistent with aromatic stacking (~3.5 Å). Remarkably, these π-stacking interactions appear to be symmetrical, occurring on both sugar rings, likely contributing to the stabilization of a preferred, low-energy conformation. The presence of well-defined regions of electronic density, combined with a stable conformation supported by intramolecular interactions, may influence the interaction of compound *9* with biological targets. However, theoretical analysis does not provide evidence of biological selectivity. These findings support further structural and mechanistic investigation of compound *9* (Figure 5).

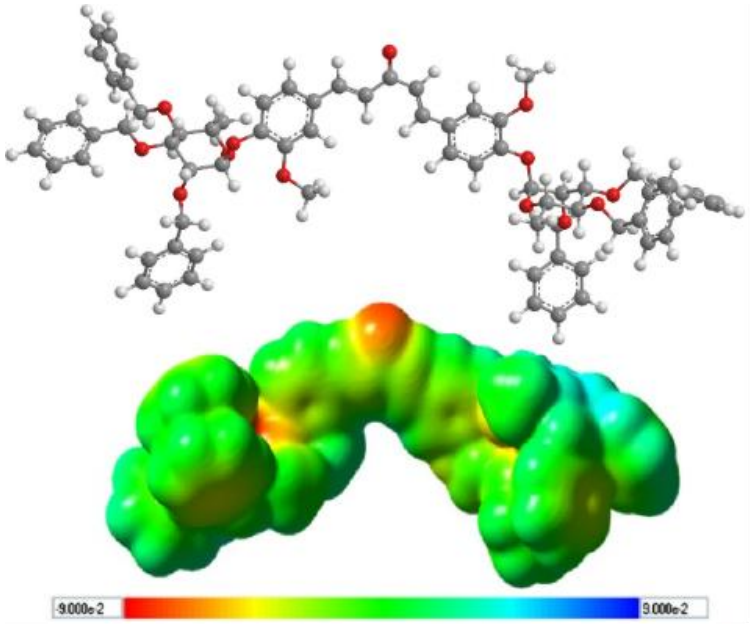


Figure 5: Electrostatic potential mapped onto the Connolly surfaces calculated for compound 9. Negative electrostatic potential regions are represented in red color (high electronic density) while positive electrostatic potential areas are shown in dark blue color (low electronic density).

3.7 Target fishing

SEA research centers gives two parameters for the evaluations of target fishing studies, the first is a P-value, which reflects the statistical significance of the similarity enrichment generated by the SEA algorithm [9], the second is a max-TC, also known as Tanimoto coefficient, it compares the molecule in being studied to known ligands in the dataset and gives a number between 0 and 1 based on how similar those are, the higher the number the more identical the

molecules are [17]. Results show that Stromal cell-derived factor 1 (CXCL12) was identified as a putative association for compound *9*, with a p-value of 1.274 e-73, indicating high statistical significance of the SEA similarity enrichment. The Tanimoto coefficient value was 0.36, indicating modest structural similarity between compound *9* and known ligands in the dataset.

Stromal cell-derived factor 1, also known as CXCL12 is a chemokine expressed in many cells and tissues, its main function is to activate leukocytes. When stimulated by TNF or IL1 [18, 19], it also has an important function in angiogenesis in adults [20], for this study its relevancy is that its connected to the invasiveness and migration of breast cancer cells, the subject of this paper.

According to Liekens et al. (2010) [21], cancer cells may overexpress CXCL12, this unregulated production of the chemokine alters the microenvironment through paracrine signaling, leading to tumor growth. CXCL12 has also been found to be present on the angiogenic process of tumor cells, the creation of new blood vessels, leading to a more vascularized tumor, boosting its growth and potential for metastasis.

Taken together, these studies suggest a putative computational association between compound *9* and CXCL12-related ligand sets; this result does not demonstrate direct interaction with CXCL12 or modulation of angiogenesis, metastasis, or the tumor microenvironment. Although the low Tanimoto coefficient indicates molecular differences compared to ligands on the database, the low P-value supports the statistical significance of the SEA association, whereas target validation requires additional experimental procedures. Further experimental procedures are warranted.

4. CONCLUSION

In this study, a new *O*-glycosylated pentadienone (compound 9) derived from curcumin was evaluated as a potential antitumor agent against human breast cancer cells. Compound *9* exhibited moderate cytotoxic activity against MCF-7 cells; however, comparison with curcumin is based on literature values obtained under different experimental conditions and should not be interpreted as a direct experimental superiority. Mitochondrial membrane depolarization and cytochrome c release were compatible with involvement of the intrinsic mitochondrial apoptotic pathway, but do not definitively establish apoptosis on their own. Importantly, compound *9* displayed greater cytotoxicity toward FN-1 fibroblasts than toward MCF-7 cells (SI = 0.40), demonstrating low tumor selectivity and representing a major limitation of the present study.

Theoretical modeling revealed a compact molecular conformation stabilized by intramolecular π–π interactions and well-defined regions of electronic density, which may contribute to its biological activity. In addition, exploratory target fishing analysis suggested a potential association with pathways involved in cell migration and angiogenesis, such as the CXCL12 axis, providing hypotheses for future mechanistic investigations. Furthermore, compound *9* altered the MTT-derived metabolic activity/viability signal in murine macrophages without evidence of cytotoxicity under the tested conditions, warranting further functional investigation.

Overall, these findings indicate that *O*-glycosylation of the pentadienone scaffold yielded a molecular prototype with cytotoxic activity that requires structural optimization, particularly to improve tumor selectivity. Future studies focused on structural refinement, target validation, and functional immunological assays will be essential to advance compound *9* toward improved efficacy and selectivity.

5. ACKNOWLEDGEMENTS

The authors are grateful to DAAD and CAPES for their financial support (Project no. PKZ: A/13/71820 – Ph.D. Fellowship). We are also grateful to FAPESP for the software's (FAPESP 2013/01875-0).

6. REFERENCES

1. Harbeck N, Penault-Llorca F, Cortes J, Gnant M, Houssami N, Poortmans P. Breast cancer. Nat Rev Dis Primers. 2019 Sep;5(1):66. doi: 10.1038/s41572-019-0111-2
2. Palma M. Advancing breast cancer treatment: The role of immunotherapy and cancer vaccines in overcoming therapeutic challenges. Vaccines (Basel). 2025 Mar;13(4):344. doi: 10.3390/vaccines13040344
3. Islam MDR, Rauf A, Akash S, Trisha SI, Nasim AH, Akter M. Targeted therapies of curcumin focus on its therapeutic benefits in cancers and human health: Molecular signaling pathway-based approaches and future perspectives. Biomed Pharmacother. 2024;170:116034. doi: 10.1016/j.biopha.2023.116034
4. Sueth-Santiago V, Mendes-Silva GP, Decoté-Ricardo D, de Lima MEF. Curcumin, the golden powder from turmeric: insights into chemical and biological activities. Quim Nova. 2015 Dec;38(4):538-52. doi: 10.5935/0100-4042.20150035
5. Kaur K, Al-Khazaleh AK, Bhuyan DJ, Li F, Li CG. A review of recent curcumin analogues and their antioxidant, anti-inflammatory, and anticancer activities. Antioxidants. 2024 Sep;13(9):1092. doi: 10.3390/antiox13091092
6. Paulraj F, Abas F, Lajis N, Othman I, Hassan S, Naidu R. The curcumin analogue 1,5-bis(2-hydroxyphenyl)-1,4-pentadiene-3-one induces apoptosis and downregulates E6 and E7 oncogene expression in HPV16 and HPV18-infected cervical cancer cells. Molecules. 2015 Jun;20(7):11830-60. doi: 10.3390/molecules200711830
7. Sharon N, Lis H. Lectins: cell-agglutinating and sugar-specific proteins. Science. 1972 Sep;177(4053):949-59. doi: 10.1126/science.177.4053.949
8. Lee EJ, Jang KH, Im SY, Lee YK, Farooq M, Farhoudi R. Physico-chemical properties and cytotoxic potential of Cordyceps sinensis metabolites. Nat Prod Res. 2015 Aug;29(5):455-9. doi: 10.1080/14786419.2014.948438
9. Keiser MJ, Roth BL, Armbruster BN, Ernsberger P, Irwin JJ, Shoichet BK. Relating protein pharmacology by ligand chemistry. Nat Biotechnol. 2007 Feb;25(2):197-206. doi: 10.1038/nbt1284
10. Hu S, Xu Y, Meng L, Huang L, Sun H. Curcumin inhibits proliferation and promotes apoptosis of breast cancer cells. Exp Ther Med. 2018 Aug;16(2):1266-72. doi: 10.3892/etm.2018.6345
11. Zargan S, Salehi Borough M, Zargan J, Shayesteh M, Haji Noor Mohammadi A, Mousavi M, et al. Evaluation of the anti-cancer effect of curcumin on MCF-7 cells in 3D culture conditions to increase the efficacy of breast cancer treatment. J Appl Biotechnol Rep. 2022;9(1):547-56. doi: 10.30491/JABR.2021.285386.1379
12. Mariño KV, Cagnoni AJ, Croci DO, Rabinovich GA. Targeting galectin-driven regulatory circuits in cancer and fibrosis. Nat Rev Drug Discov. 2023;22:295-316.
13. Kuzminska J, Szyk P, Mlynarczyk DT, Bakun P, Muszalska-Kolos I, Dettlaff K, et al. Curcumin derivatives in medicinal chemistry: Potential applications in cancer treatment. Molecules. 2024;29(22):5321. doi: 10.3390/molecules29225321
14. Nagargoje AA, Khedkar VM, Shingate BB. Anticancer perspectives of monocarbonyl analogs of curcumin: A decade (2014–2024) review. Arch Pharm (Weinheim). 2024;357:e2400197. doi: 10.1002/ardp.202400197
15. Green DR. The mitochondrial pathway of apoptosis: Part I: MOMP and beyond. Cold Spring Harb Perspect Biol. 2022 May;14(5):a041038. doi: 10.1101/cshperspect.a041038
16. Hüttemann M, Pecina P, Rainbolt M, Sanderson TH, Kagan VE, Samavati L, et al. The multiple functions of cytochrome c and their regulation in life and death decisions of the mammalian cell: From respiration to apoptosis. Mitochondrion. 2011 May;11(3):369-81. doi: 10.1016/j.mito.2011.01.010
17. Bajusz D, Rácz A, Héberger K. Why is Tanimoto index an appropriate choice for fingerprint-based similarity calculations? J Cheminform. 2015;7:20. doi: 10.1186/s13321-015-0069-3
18. Janssens R, Struyf S, Proost P. The unique structural and functional features of CXCL12. Cell Mol Immunol. 2018 Apr;15(4):299-311. doi: 10.1038/cmi.2017.107
19. Cambier S, Gouwy M, Proost P. The chemokines CXCL8 and CXCL12: molecular and functional properties, role in disease and efforts towards pharmacological intervention. Cell Mol Immunol. 2023 Mar;20(3):217-51. doi: 10.1038/s41423-023-00974-6
20. Sun X, Cheng G, Hao M, Zheng J, Zhou X, Zhang J, et al. CXCL12/CXCR4/CXCR7 chemokine axis and cancer progression. Cancer Metastasis Rev. 2010 Dec;29(4):709-22. doi: 10.1007/s10555-010-9256-x
21. Liekens S, Schols D, Hatse S. CXCL12-CXCR4 axis in angiogenesis, metastasis and stem cell mobilization. Curr Pharm Des. 2010;16(35):3903-20. doi: 10.2174/138161210794455003